HNUE JOURNAL OF SCIENCE
Natural Sciences 2024, Volume 69, Issue 3, pp. 35-45
This paper is available online at http://hnuejs.edu.vn/ns
DOI: 10.18173/2354-1059.2024-0033

CHARACTERIZING KAOLIN-BASED ADDITIVE FOR COMBUSTION OF SUGARCANE BAGASSE-DERIVED FUEL BY THERMAL ANALYSIS

Nguyen Truong Giang[1,*] and Mai Xuan Quang[2]
[1]*Faculty of Basic Sciences, University of Transport and Communications, Hanoi city, Vietnam*
[2]*Hung Vuong High School, Gia Lai province, Vietnam*
[*]Corresponding author: Nguyen Truong Giang, e-mail: ntgiang@utc.edu.vn

Received October 4, 2024. Revised October 24, 2024. Accepted October 31, 2024.

Abstract. In this work, the characterization of kaolin-based additives for the combustion of sugarcane bagasse-derived biomass was investigated using thermogravimetric-derivative thermogravimetric (TG-DTG) analysis and differential thermal analysis (DTA). Sugarcane bagasse powder (SB) was mixed with 2 wt.% and 4 wt.% of kaolin powder (KL) and then pressed into fuel pellets. Combustion parameters (ignition temperature T_i, burnout temperature T_b, maximum peak temperature T_{max}, ignition index C_i, burnout index C_b, comprehensive combustibility index S, and activation energy E_a) for the pellets were evaluated.

Keywords: biomass, combustion parameters, kaolin, sugarcane bagasse, thermal analysis.

1. Introduction

Currently, renewable energy is a global trend in the energy sector. Renewable energy can replace fossil energy sources (such as coal, oil, and gas), which are rapidly depleting and are the largest contributors to global climate change due to emitting large amounts of greenhouse gases. Renewable resources include solar energy, wind energy, geothermal energy, and biomass energy, among others. In particular, energy sources from biomass fuels are receiving worldwide attention today because they can be produced on large, widespread, and diverse scales [1], [2].

Biomass fuels can be in the forms of gas, liquid, and solid, derived from animals and plants, such as agricultural and forestry waste, animal waste, urban sludge, municipal waste, etc. [3]. Biomass fuels have been used for a long time as fuel for cooking and heating. Currently, biomass fuels derived from wastes are gaining the most attention, not only helping to utilize a large amount of renewable energy from waste sources but also reducing environmental pollution [1]-[4].

Vietnam currently has a large source of sugarcane bagasse (about 7.8 million tons a year) and more than 40 power generation projects for using bagasse-based fuel [5]. In addition, the government's support and facilitation policies (for example, Decision No. 08/2020/QD-TTg on increasing electricity purchase prices from biomass projects for heat and power generation) provide favorable opportunities for businesses to invest in technology and equipment for generating electricity. Therefore, in recent years, sugar companies have invested in new or upgraded equipment for producing electricity from the combustion of this fuel [6].

However, when using biomass fuels like sugarcane bagasse, issues such as slag-ash adhesion and fusion inside the combustion chamber system must be addressed. This is because biomass contains elemental constituents of alkaline and alkaline earth metals (for example K, Na) [7], which are released in vapor-phase compounds (such as KCl, K_2SO_4, K_2CO_3, KOH) during the combustion process at temperatures ranging from 700 ÷ 1000 ^oC. These compounds can combine with other volatile compounds from the combustion process to create adhesion and fusion compounds. This slag ash accumulates and agglomerates inside the furnace chamber, heat exchanger, and tubes, forming sticky residues that are very difficult to clean or remove [4], [8]. Therefore, this causes system blockage, energy loss, reduced thermal-energy conversion efficiency, and corrosion [8], [9]. To reduce or eliminate these slag-ash adhesions and fusions, additives based on inorganic materials from ore/mineral sources such as clay (typically kaolin), limestone, dolomite, etc., can be mixed into biomass fuel for combustion. These are effective approaches that have been investigated [10], [11]. This is achieved by the additive materials being able to provide two functions: (i) catalyzing the fuel combustion reactions, and (ii) creating chemical reactions with K/Na-based compounds to form compounds with high melting points (> 900 ^oC), thereby favorably forming bottom ashes and reducing slag-ash agglomeration and fusibility inside the system [12].

Kaolin is a clay whose main component is the mineral kaolinite, with the typical formula $Al_2Si_2O_5(OH)_4$ [8]. In crude clay, kaolin can contain other oxides (such as SiO_2, Fe_2O_3, TiO_2) or impurity elements (such as K, Na, Ca, Fe) in the crystal structure of Kaolinite. With this characteristic, kaolin is known to be an effective mitigator of slag-ash agglomeration and fusibility for biomass fuel combustion by creating compounds with high melting points, as reported in Refs. [4], [8], [12]. However, currently, there are relatively few publications on kaolin-derived additives serving as catalysts for fuel combustion reactions.

In this work, kaolin clay was used as an additive to promote the combustion of sugarcane bagasse. Combustion parameters were calculated by thermal analysis (TG-DTG and DTA), aiming to investigate aspects related to using biomass and mineral-based materials (such as sugarcane bagasse and kaolin clay) for clean and renewable energy from biomass fuels.

2. Content

2.1. Experiments

A sample of sugarcane bagasse (originated from the northern province of Hoa Binh) was dried at 100 ^{o}C for 1 hour, ground using a blade grinder, and then sieved (35 mesh) to obtain a bagasse powder. Organic elemental constituents (C, H, N, S, O) of the bagasse powder were analyzed by FlashSmart™ Elemental Analyzer (Thermo Scientific). A sample of kaolin clay (originated from the northern province of Yen Bai and under the typical refining process) was dried at 100^{o}C for 1 hour, ground with a ball mill, and then sieved (325 mesh) to obtain fine kaolin powder. The morphology and crystal phases of the kaolin powder samples were examined by scanning electron microscopy (SEM, Hitachi S-4800) and X-ray diffraction (XRD, Bruker D8). Inorganic elemental constituents of the kaolin powder were analyzed by X-ray fluorescence (XGT-9000, Horiba).

The bagasse powder was mixed with 2.0 wt.% and 4.0 wt.% of the kaolin powder. Then, these mixtures were pressed into pellets using a hydraulic press at a condition of pressure of 5000 psi and temperature of 120 ^{o}C to get cylindrical fuel pellets with a diameter of 12 mm. Corresponding to the used kaolin contents, the fuel pellet samples fabricated from bagasse, bagasse + 2.0 wt.% kaolin, and bagasse + 4.0 wt.% kaolin were denoted as SB, SB+2KL, and SB+4KL, respectively. Figure 1 shows representative images of the samples of dried sugarcane bagasse, sugarcane bagasse powder, kaolin powder, and fuel pellets.

Figure 1. Images of the samples of dried sugarcane bagasse (a), sugarcane bagasse powder (b), kaolin powder (c) and fuel pellets (d)

To determine moisture content (%M), volatile organic content (%VOC), fixed carbon content (%FC), and ash content (%Ash) of the fuel pellets, a furnace (FUW210PA, Advantec) was used to dry and calcine the fuel samples according to standard procedures for biomass materials, including ISO 18134-3:2015, ISO 1171:2010, and BS 1016-104.4:1998. Specifically, to determine moisture content, an amount of the material sample (≥ 1 g) was weighed and placed into a crucible. The total mass was weighed, and the material crucible was dried at 105 °C for 3 hours, then reweighed. The moisture content (%M) was calculated from the mass lost during this procedure. After this 105 ^{o}C drying procedure, the material crucible was heated according to the following temperature program: increased evenly to 250 °C in 30 minutes and maintained for 60 minutes, continued to increase evenly to 550 °C in 30 minutes, and

maintained for 120 minutes. The crucible was then cooled naturally and weighed to determine the mass lost due to evaporation, thereby determining the volatile organic content (%VOC). To determine the ash content, the material crucible (under the 105 ^{o}C drying process above) was heated according to the following program: increased evenly to 500 °C in 60 minutes and maintained for 30 minutes, then increased evenly to 815 °C and maintained 60 minutes. The crucible was cooled naturally and reweighed to calculate the mass remaining in the crucible (ash weight), thus determining the ash content (%Ash). The fixed carbon content was calculated as %FC = 100 - %M - %VOC - %Ash.

The fuel pellet samples of SB, SB+2KL, and SB+4KL were analyzed by thermogravimetric analysis - TG and differential thermogravimetric analysis - TGA (using Thermo plus EVO2/TG-DTA8121, Rigaku) under a condition of heating rate of 20 ^{o}C/min and a temperature range of 30 ÷ 900 ^{o}C in an air ambient.

2.2. Results and discussion

Table 1 shows the results of the ultimate analysis of the organic elemental contents (C, H, N, S, O) of SB and the inorganic elemental contents of KL. It was observed that carbon (C) and oxygen (O) were the large proportions in SB, with contents of 47.75 wt.% and 46.01 wt.%, respectively. Hydrogen (H) and nitrogen (N) were present in lower proportions, with contents of 5.83 wt.% and 0.40 wt.%, respectively, while sulfur (S) could not be detected in this case. The proximate analysis of KL showed that silicon (Si) and aluminum (Al) are the typical main elements of kaolin clay, with high contents of 45.23 at.% and 31.01 at.%, respectively. In addition, the results indicated that KL contained other impurity elements such as potassium (K), iron (Fe), magnesium (Mg), and titanium (Ti) with small contents of 11.19 at.%, 7.91 at.%, 1.55 at.%, and 0.81 at.%, respectively. These impurity elements are consistent with the golden-brown color of the kaolin powder, as seen in Figure 1c.

Table 1. Ultimate analysis of the samples of sugarcane bagasse and kaolin clay

Samples	Elements	Content
Sugarcane bagasse	C	47.75 (wt.%)
	O	46.01 (wt.%)
	H	5.83 (wt.%)
	N	0.40 (wt.%)
	S	-
Kaolin clay	Si	45.23 (at.%)
	Al	31.01 (at.%)
	K	11.19 (at.%)
	Fe	7.91 (at.%)
	Mg	1.55 (at.%)
	Ti	0.81 (at.%)
	-	2.30 (at.%)

Table 2 shows the results of the proximate analysis of the pellet samples with contents of moisture (%M), volatile organic compounds (%VOC), fixed carbon (%FC), and ash (%Ash). The results indicated that all the pellet samples were primarily composed of volatile organic compounds, with approximately 90 wt.% of the total mass. The moisture contents of the samples were small, about 5.46 - 6.20 wt.%, due to the processes of drying at 100 °C and pressing at 120 °C into pellets. The fixed carbon content and ash content presented slight increases with the addition of kaolin content.

Table 2. Proximate analysis of the pellet samples

Proximate analysis (wt.%)	**Pellet samples**		
	SB	***SB+2KL***	***SB+4KL***
%M	6.20	5.57	5.46
%VOC	90.92	90.85	89.97
%FC	0.44	0.52	0.55
%Ash	2.45	3.06	4.02

SEM image and XRD pattern of the kaolin powder are shown in Figure 2. It was observed that the morphology of the kaolin powder was relatively homogeneous with a leaf-shaped structure, which is typical of natural kaolin clay. This characteristic was similar to the results reported in ref. [13]. Crystal structures of the kaolin powder were found to include three main phases: two typical minerals in clay, Kaolinite - $Al_2Si_2O_5(OH)_4$ (PDF 00-058-2006) and Muscovite - $KAl_2(Si,Al)_4(OH)_2$ (PDF 00-058-2035), and another of quartz - SiO_2 (PDF 01-079-1910).

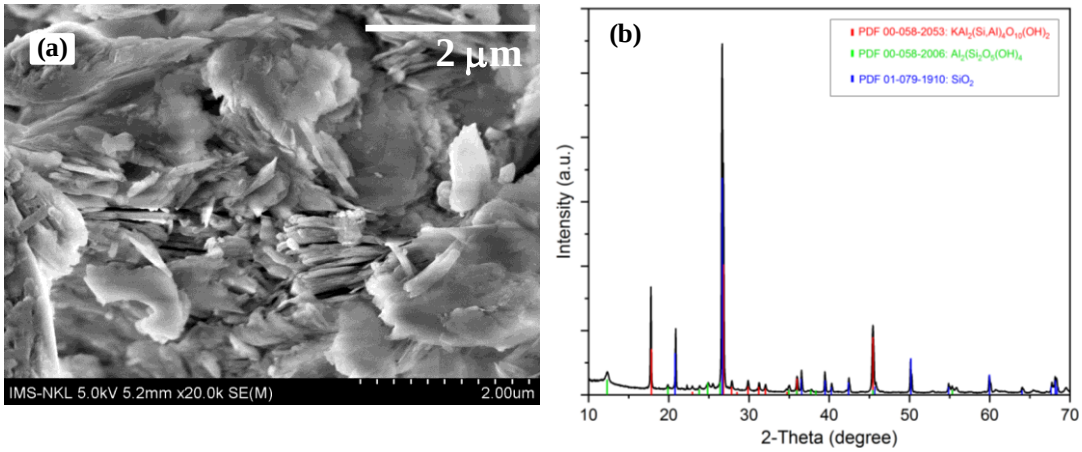

Figure 2. SEM image (a) and XRD pattern (b) of the kaolin powder

Figure 3 shows the results of thermogravimetric analysis (TG) and differential thermogravimetric analysis (DTA) of the pellet samples of SB, SB+2KL, and SB+4KL. This result presented that TG-DTA curves were quite similar and represented the combustion characteristic of biomass fuel type (SB). Herein, it was found that the water evaporation could occur in the low-temperature region (with an endothermic peak < 100 ^oC), and the decomposition-combustion reactions in the high-temperature region of 300 ÷ 800 ^oC (with two exothermic peaks). The two exothermic peaks (indicated in DTA curves) at

about 340 °C and 435 °C are in corresponding with the two regions of the high mass loss (on TG curves). The two exothermic peaks represented combustible reactions of two organic groups of SB to be "cellulose and hemicellulose" at low temperature (340 °C) and "lignin" at high temperature (435 °C). It was noted that the temperature of the lignin combustion peak tended to decrease with increasing kaolin content, while that of the cellulose and hemicellulose combustion peaks changed only slightly. However, the high value of the exothermic peak of the cellulose and hemicellulose combustion changed strongly and sharply when the kaolin content increased in the pellet sample.

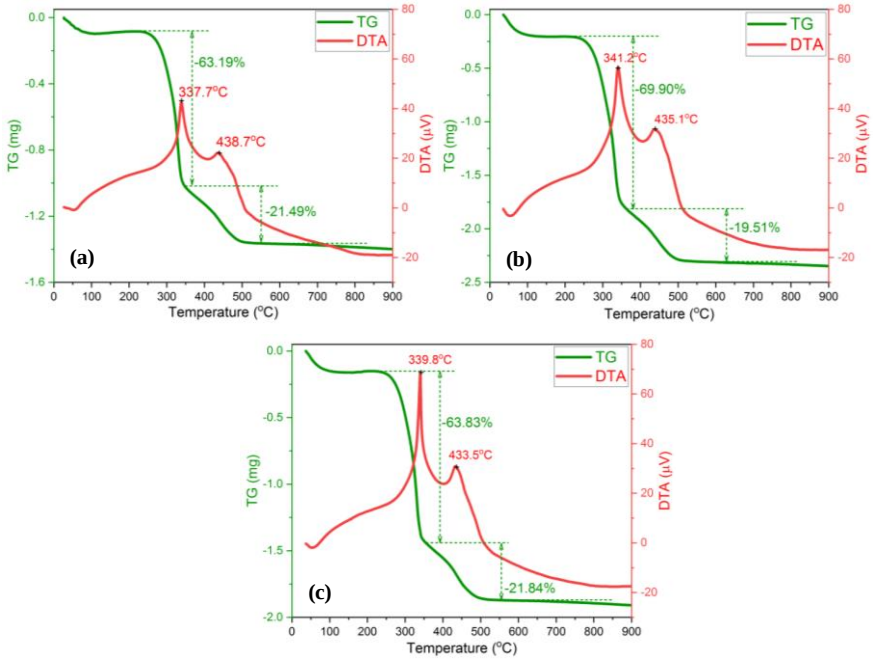

Figure 3. TG-DTA curves of the pellets of BM (a), BM+2KL (b), and BM+4KL (c)

For kinetic analysis, several models can be used, such as the Coats–Redfern model, Kissinger–Akahira–Sunose model, Flynn–Wall–Ozawa model, Starink model, Tang model, and Friedman model [13]-[15]. In this work, thermogravimetric (TG) data were used to calculate and apply the Coats–Redfern model for determining the combustion activation energy (Ea) for the pellet samples, as follows:

$$\frac{d\alpha}{dt} = k(T)\, f(\alpha) \tag{1}$$

where T is the absolute temperature (K), $k(T)$ is the reaction rate constant, t is the reaction time (min), $f(\alpha)$ is the reaction mechanism function, α is the conversion rate, and $f(\alpha)$ represents the reaction mechanism function, which can be written as $f(\alpha) = (1 - \alpha)^n$, n is the reaction order. $k(T)$ is expressed according to the Arrhenius equation:

$$k(T) = A\exp\left(-\frac{E_a}{RT}\right) \tag{2}$$

where R is the gas constant, A is the pre-exponential factor (min^{-1}), E_a is the combustion activation energy (kJ/mol), and R is the universal gas constant (8.314 J/(mol K)). The conversion rate (α) of material in the combustion process is defined according to the following equation:

$$\alpha = \frac{m_0 - m_t}{m_0 - m_f} \tag{3}$$

where m_o is the initial mass of the sample (mg), m_t is the mass of the sample at time t (mg) and m_f is the final mass of the sample (mg). The constant heating rate β under the non-isothermal combustion can be expressed as:

$$\beta = \frac{dT}{dt} \tag{4}$$

To combine Eqs. (4), (3), and (2) into Eq. (1), the following Eq. (5) can be obtained:

$$\frac{d\alpha}{dT} = \frac{1}{\beta}\frac{d\alpha}{dt} = \frac{1}{\beta}A\exp\left(-\frac{E_a}{kT}\right)(1-\alpha)^n \tag{5}$$

Integrating Eq. (5) and simplifying with the conditions of $E_a/RT \geq 1$ and $(1 - 2RT/E_a) \approx 1$, the following equations (Coats and Redfern) are obtained as:

$$Y = \ln\left[\frac{-\ln(1-\alpha)}{T^2}\right] = \ln\left(\frac{AR}{\beta E_a}\right) - \frac{E_a}{RT}, (n=1) \tag{6}$$

$$Y = \ln\left[\frac{1-(1-\alpha)^{1-n}}{T^2(1-n)}\right] = \ln\left(\frac{AR}{\beta E_a}\right) - \frac{E_a}{RT}, (n\neq 1) \tag{7}$$

Thus, from Eqs. (6) and (7), the activation energy (E_a) can be obtained through the slope of the regression lines by plotting $Y = \ln[-\ln(1-\alpha)/T^2]$ and $Y = \ln[[1-(1-\alpha)^{1-n}]/[T^2(1-n)]]$ ($n\neq1$) versus $1/T$.

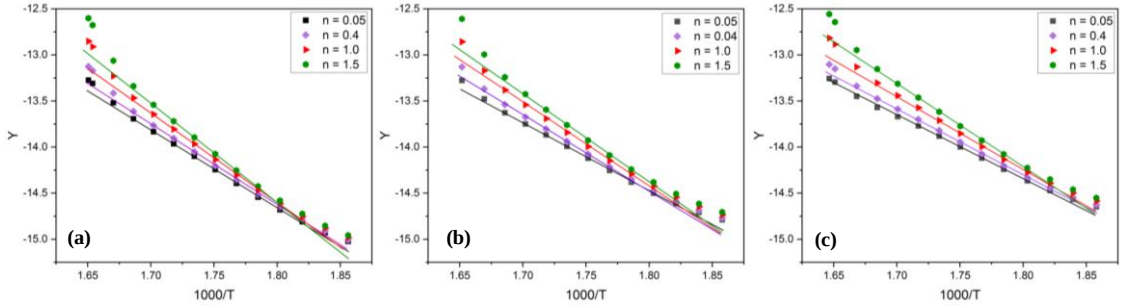

Figure 4. Illustration of typical results of the calculated data points and the linear fitting curves of Y function versus 1000/T when varying n values for the samples of SB (a), SM+2KL (b) and SB+4KL (c)

Figure 4 illustrates the results of the data points calculated from experimental data (TG-DTG) and shows the linear dependent lines of Y on 1000/T when changing different values n for the samples of SB, SB+2KL, and SB+4KL. It was found that all three samples showed a good linear dependence of the data points when n was in the small value range ($n \leq 0.5$), and the linearity gradually decreased when n was larger values. Magnitudes of the activation energy (E_a) were calculated according to the slope value of the linear fitting lines ($R^2 > 0.99$), as the results are shown in detail in Table 3. It could be seen that the activation energy E_a gradually decreased from 74.5 kJ/mol to 62.5 and 59.4 kJ/mol when changing from SB to SB+2KL and SB+4KL, respectively.

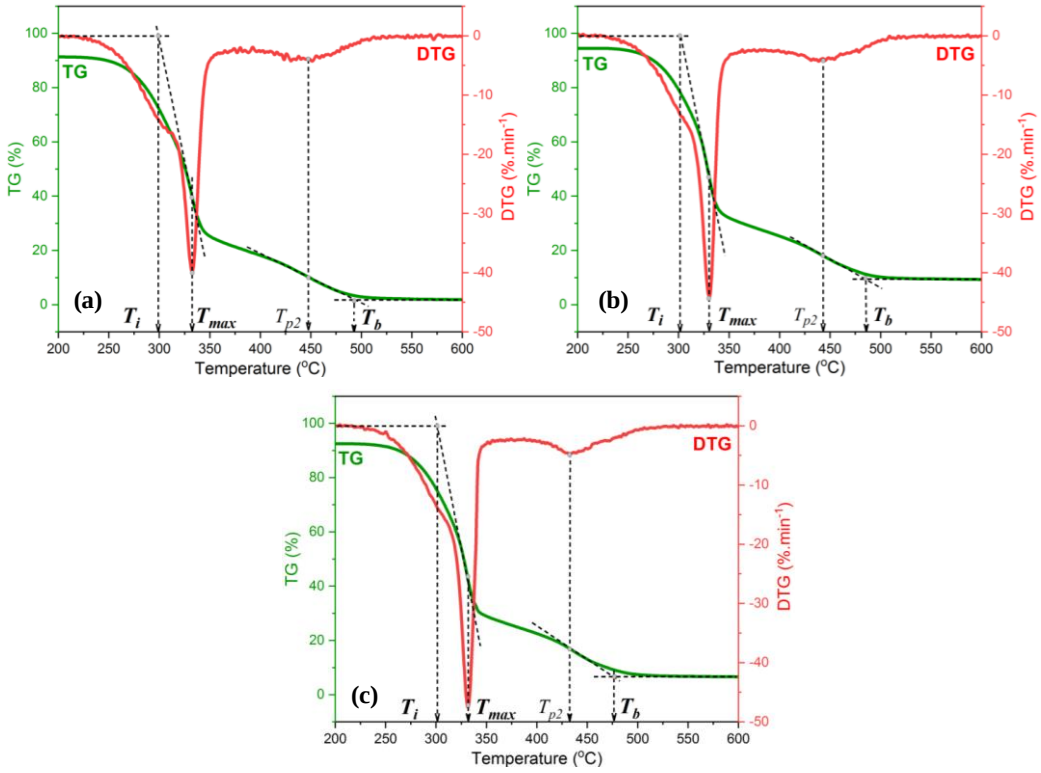

Figure 5. TG-DTG curves and the method for determining combustion parameters of the pellet samples of SB (a), SM+2KL (b), and SB+4KL (c)

For further combustion analysis, TG-DTG curves were used to evaluate the characteristic combustion parameters of the pellet samples. In detail, the combustion temperature parameters including ignition temperature T_i (°C), burnout temperature T_b (°C), second-peak temperature T_{p2} (°C), and maximum peak temperature T_{max} (°C) were determined by the method as indicated in Figure 5 [15]. The parameters for evaluating the combustion process include ignition index C_i (%/min^3), burnout index C_b (%/min^4), and comprehensive combustibility index S (%^{2}/°C^3.min^2). These parameters can be evaluated according to the equations [13], [15]:

$$C_i = \frac{DTG_{max}}{t_i t_{max}} \quad (8)$$

$$C_b = \frac{DTG_{\max}}{\Delta t_{1/2} t_{\max} t_b} \quad (9)$$

$$S = \frac{DTG_{\max} DTG_{av}}{T_i^2 T_b} \quad (10)$$

where DTG_{max} is the maximum mass loss rate (%/min); DTG_{av} is the average mass loss rate (%/min); t_i is the ignition time, t_{max} is the maximum peak time, $\Delta t_{1/2}$ is the time zone of DTG/DTG_{max} = 1/2, and t_b is the burnout time.

Table 3. Combustion parameters calculated from TG-DTG of the pellet samples

Parameters	Sample		
	SB	***SB+2KL***	***SB+4KL***
T_i (°C)	299.2	302.1	302.2
T_{max} (°C)	332.8	330.8	331.1
T_b (°C)	492.9	479.8	476.3
t_i (min)	14.8	15.6	15.8
t_b (min)	24.5	24.5	23.6
$\Delta t_{1/2}$ (min)	8.7	8.6	7.8
DTG_{max} (%/min)	40.1	44.2	47.4
DTG_{av} (%/min)	7.1	7.4	7.5
C_i (%/min^3.10^{-2})	16.6	16.8	19.7
C_b (%/min^4.10^{-2})	1.1	1.2	1.6
S (%^{2}/(°C^3.min^3).10^{-7})	64.3	74.7	81.6

Figure 5 shows TG-DTG curves and the method for determining the combustion parameters (T_i, T_{max}, $T_{p2,}$ and T_b) of the pellets of SB, SM+2KL, and SB+4KL. From DTG curves, it can be found that the maximum combustion peak occurred in the temperature region around 340 °C, which could be assigned to the combustion contribution of cellulose and hemicellulose. Meanwhile, the second combustion broadens peak (T_{p2}) in high temperature region (around 440 °C) was referred to as the difficult-to-burn properties of lignin. Table 4 shows details of the combustion parameters calculated from TG-DTG data of the samples of SB, SB+2KL, and SB+4KL. These results presented that the temperatures of T_i and T_{max} were not much different when compared between the samples. However, the burnout temperatures (T_b) of the samples of SB, SB+2KL, and SB+4KL were significantly different with values of 492.9 °C, 479.8 °C, and 446.3 °C, respectively. The burnout temperature decreased quietly when the pellet sample was used with the kaolin-based additive. DTG_{max} of the samples of SB, SM+2KL, and SB+4KL were strongly increased with values of 40.1, 44.2, and 47.4, respectively. The results provided that the combustion was promoted and concentrated in a narrow temperature range when

the fuel sample was added by the kaolin additive. The ignition index C_i, burnout index C_b index, and comprehensive combustibility index S of all samples presented an increasing trend with the used kaolin content in the pellet samples. Notably, the comprehensive combustibility index S had a strong increase with values of 64.3, 74.7, and 81.6 ($\%^2/(^oC^3.min^3).10^{-7}$) in correspondence with the samples of SB, SM+2KL, and SB+4KL, respectively. The characteristic suggested that the fuel combustion occurred more favourably and easily with the presence of kaolin additive. It could be concluded that kaolin contributed to a significant improvement in catalysis for fuel combustion reactions. Furthermore, it was considered that the impurity oxides composition (such as SiO_2, Fe_2O_3, and TiO_2 as similar results in ref. [13]) in the used kaolin source also contributed to this combustion performance.

3. Conclusions

This work has investigated the use of kaolin clay originating from Yen Bai as an additive for biomass fuel derived from sugarcane bagasse through thermal analysis. The analyses of TG-DTG and DTA were used to evaluate the combustion parameters. The obtained results presented the typical characteristics of biomass fuel from the sugarcane bagasse. The activation energy (E_a) decreased when the fuel pellet was added by the kaolin additives with 2.0 and 4.0 wt.%. The combustion parameters, including the ignition index (C_i), burnout index (C_b), and comprehensive combustibility index (S) significantly improved when the fuel pellets were used with the additive. In addition to its inherent role in mitigating slag-ash agglomeration and fusibility, this work demonstrated that kaolin clay could also promote the combustion of sugarcane bagasse-derived biomass fuel.

Acknowledgements. This research is funded by the University of Transport and Communications (UTC) under grant number T2024-CB-004.

REFERENCES

[1] Danso BE & Osei W, (2022). Bioenergy and biofuel production from biomass using thermochemical conversions technologies - A review. *AIMS Energy*, 10, 585-647.

[2] Ahmmad F, Sohel M, Islam M, Ani FN & Tahzinul, (2020). Development of a Pelletizing Process to Improve the Properties of Biomass Pellets. *Advances in Engineering Research*, 198, 337-343.

[3] Tripathi M, Sahu JN & Ganesan P, (2016). Effect of process parameters on production of biochar from biomass waste through pyrolysis: A review. *Renewable and Sustainable Energy Reviews*, 55, 467-481.

[4] Mack R, Kuptz D, Schon C & Hartmann H, (2019). Combustion behavior and slagging tendencies of kaolin additivated agricultural pellets and of wood-straw pellet blend in a small-scale boiler. *Biomass and Bioenergy*, 125, 50-62.

[5] Petro Vietnam Power Corporation, (2014, October). *40 projects to generate electricity from sugarcane bagasse* (in Vietnamese). https://pvpower.vn/vi/post/da-co-40-du-an-phat-dien-tu-ba-mia-1772.htm.

[6] Vietnam Agriculture Newspaper, (2021, December). *Energy-saving electricity production from sugarcane bagasse* (in Vietnamese). https://nongsanviet.nongnghiep.vn/san-xuat-dien-tu-ba-mia-tiet-kiem-nang-luong-d310694.html.

[7] Lachman J, Balas M, Lisy M, Lisa H, Milcak P & Elbl P, (2021). An overview of slagging and fouling indicators and their applicability to biomass fuels. *Fuel Processing Technology*, 217, 106804.

[8] Maj I & Matus K, (2023). Aluminosilicate Clay Minerals: Kaolin, Bentonite, and Halloysite as Fuel Additives for Thermal Conversion of Biomass and Waste. *Energies*, 16(11), 4359.

[9] Bartels M, Lin W, Nijenhuis J, Kapteijn F & Ommen JRv, (2008). Agglomeration in fluidized beds at high temperatures: mechanisms, detection and prevention. *Progress in Energy and Combustion Science*, 34, 633-666.

[10] Najser J, Mikeska M, Peer V, Frantík J & Kielar J, (2020). The addition of dolomite to the combustion of biomass fuel forms: the study of ashes agglomeration and fusibility. *Biomass Conversion and Biorefinery*, 10, 471-481.

[11] Morris JD, Daood SS & Nimmo W, (2022). The use of kaolin and dolomite bed additives as an agglomeration mitigation method for wheat straw and miscanthus biomass fuels in a pilot-scale fluidized bed combustor. *Renewable Energy*, 196, 749-762.

[12] Gollmer C, Weigel V & Kaltschmitt M, (2023). Emission Mitigation by Aluminum-Silicate-Based Fuel Additivation of Wood Chips with Kaolin and Kaolinite. *Energies*, 16, 3095.

[13] Wang Z, Hong C, Xing Y, Li Y, Feng L & Jia M, (2018). Combustion behaviors and kinetics of sewage sludge blended with pulverized coal: With and without catalysts. *Waste Management*, 74, 288-296.

[14] Sukirti D, Rakesh K & Monoj KM, (2022). Pyrolysis kinetics and thermodynamics of pomegranate peel usingTG/DTG analysis. *Biomass Conversion and Biorefinery*, 14, 12411-12425.

[15] Sun Y, Sun H, Yang T, Zhu Y & Li R, (2024). Combustion Characterization and Kinetic Analysis of Mixed Sludge and Lignite Combustion. *ACS Omega*, 9, 6912-6923.